Available online at www.sciencedirect.com
SCIENCE DIRECT®
Nonlinear Analysis 63 (2005) e345–e356
Nonlinear Analysis
www.elsevier.com/locate/na

A time-accurate pseudo-wavelet scheme for parabolic and hyperbolic PDE's

B.V. Rathish Kumar*, Mani Mehra

Department of Mathematics, Indian Institute of Technology, Kanpur 208 016, India

Abstract

In this paper, we propose wavelet Taylor–Galerkin schemes for parabolic and hyperbolic PDEs taking full advantage of the compression properties of wavelet basis. The discretization in time is performed before the spatial discretization by introducing high-order generalization of the standard time-stepping schemes with the help of Taylor series expansion in time step. Then, we present numerical results for a convection problem in one dimension and Gaussian translating hill problem in two dimensions. Finally, results for the two-dimensional turbulence are shown.

Keywords: Taylor–Galerkin method; Wavelets; Time-marching scheme; Navier–Stokes equation; Turbulence

1. Introduction

The application of methods based on wavelets to the numerical solution of partial differential equations (PDEs) has recently been studied both from the theoretical and the computational point of view due to its attractive feature: orthogonality, arbitrary regularity, good localization wavelet bases seem to combine the advantages of both spectral and finite element basis. Schematically, the wavelet-based methods for PDEs can be separated into three classes.

In a first class, wavelets are used, in the framework of a classical grid adaptive numerical code, to detect where the grid has to be refined or coarsened to optimally represent the

* Corresponding author. Tel.: +91 512 2597660; fax: +91 512 2597500
E-mail addresses: bvrk@iitk.ac.in (B.V.R. Kumar), manimeh@iitk.ac.in (M. Mehra).

0362-546X/$ - see front matter © 2005 Elsevier Ltd. All rights reserved.
doi:10.1016/j.na.2005.02.110

solution. Instead of expanding the solution in terms of wavelets, the wavelet transform is used to determine the adaptive grid [7].

In a second class, multiresolution analysis and their associated scale function bases may be used as alternative bases in Galerkin methods [1,6,11]. Such methods have thus convergence properties similar to those of spectral methods, and simultaneously partial derivative operators discretize similarly as in finite difference methods. However, as these methods do not use wavelets but rather scale function as basis functions, they cannot be adaptive methods and cannot significantly reduce the number of degree of freedom in a numerical code.

The third class, the only one which uses the compression properties of wavelet bases, contain specific wavelet methods for PDEs. In the literature, many tentatives have been performed, often based on Galerkin or Petrov–Galerkin methods. Some of them take advantage of the wavelet compression of the solution [9], others instead use the wavelet compression of the operator [5]. The aim of the present paper is to introduce the wavelet Taylor–Galerkin method which has the benefit of both the properties. In the conventional numerical approach to transient problems, the accuracy gained in using the high-order spatial discretization is partially lost due to the use of low-order time discretization schemes. Here usually spatial discretization precedes the temporal discretization. On the contrary, the reversed order of discretization can lead to better time-accurate schemes with improved stability properties. The fundamental concept behind the Taylor–Galerkin approach is to incorporate more analytical information into the numerical scheme in the most direct and natural way, so that the technique may be regarded as an extension of the Obrechkoff methods to PDEs [8] for ordinary differential equations. Higher-order accurate versions of the Euler time-stepping algorithms are developed on the basis of Taylor series expansion where the time derivatives are evaluated from the governing equation. It can be generalized to any time-stepping scheme based on Taylor series expansion.

The nonlinear or variable coefficient term is evaluated by a pseudowavelet technique. Spatial approximation can be made by using different wavelet bases such as orthogonal Daubechies wavelets [3], biorthogonal spline wavelets [2], interpolates [4], etc. Our method works with any of these basis functions. In this paper, we demonstrate our method using Daubechies compactly supported wavelets.

2. Wavelet Taylor–Galerkin method (WTGM) for evolutionary problems

In the following, we give a brief introduction to wavelets and the notation used. We first deal with one-dimensional wavelets and then consider two variants for its generalization to the multivariate case. Finally, we describe how compression properties wavelets can be used in WTGM scheme for convection problem in one dimension and multidimensional problems.

2.1. Univariate wavelets

The class of compactly supported wavelet bases was introduced by Daubechies [3] in 1988. They are an orthonormal basis for functions in $L^2(R)$. A "Wavelet System" consists

of the function $\phi(x)$ and the function $\psi(x)$ is referred to as the wavelet function. We define translates of $\phi(x)$ as

$$\phi_i(x) = \phi(x - i). \tag{2.1}$$

Multiresolution analysis (MRA) is the theory that was used by Ingrid Daubechies to show that for any nonnegative integer n there exists an orthogonal wavelet with compact support such that all the derivatives upto an order n exist. MRA describes a sequence of nested approximation spaces V_j in $L^2(R)$ such that the closure of their union equals $L^2(R)$. MRA is characterized by the following axioms

$$\{0\} \subset \cdots \subset V_{-1} \subset V_0 \subset V_1 \cdots \subset L^2(R),$$

$$\overline{\bigcup_{j=-\infty}^{j=\infty} V_j} = L^2(R),$$

$$\bigcap_{j \in Z} V_j = 0,$$

$$f \in V_j \text{ if and only if } f(2(.)) \in V_{j+1},$$

$$\phi(x - k)_{k \in Z} \text{ is an orthonormal basis for } V_0. \tag{2.2}$$

We define W_j to be the orthogonal complement of V_j in V_{j+1}, i.e. $V_j \perp W_j$ and

$$V_{j+1} = V_j + W_j, \tag{2.3}$$

$\phi_{j,k}(x) = 2^{j/2}\phi(2^j x - k)_{k \in Z}$ is an orthonormal basis for V_j and ϕ is the solution of so-called scaling equation

$$\phi(x) = \sqrt{2} \sum_{k=0}^{D-1} a_k \phi(2x - k) \tag{2.4}$$

with explicitly known coefficients a_k (low pass filter). An analytical description of ϕ is not available and also not needed. Wavelets are also dilates/translates of a single function ψ such that $\psi_{j,k} = 2^{j/2}\psi(2^j x - k)_{k \in Z}$ is an orthonormal basis for W_j. Each member of the wavelet family is determined by the dilation equation

$$\psi(x) = \sqrt{2} \sum_{k=0}^{D-1} b_k \phi(2x - k), \tag{2.5}$$

where D is the order of wavelet and $b_k = (-1)^k a_{D-1-k}$, $k = 0, 1, \ldots, D - 1$. As pointed out by Meyer (1990) the complete toll box built in $L^2(R)$ can be used in the periodic case $L^2([0, 1])$ by introducing a standard periodization technique. This technique consists at each scale in folding, around the integer values, the wavelet $\psi_{j,k}$ and the scaling functions $\phi_{j,k}$ centered in [0,1]. It writes $\tilde{\phi}_{j,l}(x) = \sum_{n=-\infty}^{\infty} \phi_{j,l}(x + n)$ and $\tilde{\psi}_{j,l}(x) = \sum_{n=-\infty}^{\infty} \psi_{j,l}(x + n)$ and generates V_{Pj} and W_{Pj}. A function $f \in V_{Pj}$ in pure periodic

scaling function expansion $f(x) = \sum_{k=0}^{2^j-1} c_k^j \tilde{\phi}_{j,k}(x)$ and the periodic wavelet expansion $f(x) = \sum_{k=0}^{2^{J_0}-1} c_k^{J_0} \tilde{\phi}_{J_0,k}(x) + \sum_{j=J_0}^{J-1} \sum_{k=0}^{2^j-1} d_k^j \tilde{\psi}_{j,k}(x)$, where J_0 satisfies $0 \leqslant J_0 \leqslant J$ and the decay of the wavelet coefficient is given by the following theorem [10]:

Theorem. *Let $P = D/2$ be the number of vanishing moments for a wavelet $\psi_{j,k}$ and let $f \in C^P(R)$. Then the wavelet coefficients decay as $|d_{j,k}| \leqslant C_P 2^{-j(P+1/2)} \max_{\xi \in I_{j,k}} |f^{(P)}(\xi)|$.*

2.2. Multivariate wavelets

The simplest way to obtain multivariate wavelets is to employ anisotropic or isotropic tensor products.

(MRA-d) Here, the multivariate wavelets are defined by

$$\psi_{j,l}(x) := \psi_{(j_1,l_1)}(x_1). \cdots .\psi_{j_d,l_d}(x_d), \quad j := (j_1, \ldots, j_d) \quad x, l \text{ analogous}$$

(MRA) Here, anisotropy is avoided. The scaling functions are simply the tensor products of the univariate scaling functions. A two-dimensional MRA can be constructed from the following decomposition:

$$\begin{aligned} \boldsymbol{V}_j &= V_j \otimes V_j \\ &= (V_{j-1} \oplus W_{j-1}) \otimes (V_{j-1} \oplus W_{j-1}) \\ &= (W_{j-1} \otimes W_{j-1}) \oplus (W_{j-1} \otimes V_{j-1}) \oplus (V_{j-1} \otimes W_{j-1}) \oplus V_{j-1} \otimes V_{j-1} \\ &= \boldsymbol{W}_{j-1} \oplus \boldsymbol{V}_{j-1}. \end{aligned}$$

Then we have $\boldsymbol{V}_J = \boldsymbol{W}_{J-1} \oplus \cdots \oplus \boldsymbol{W}_0 \oplus \boldsymbol{V}_0$. The wavelet basis is given by

$$\{\psi_{j,k} \otimes \psi_{j,l}, \psi_{j,k} \otimes \phi_{j,l}, \phi_{j,k} \otimes \psi_{j,l}\}_{k,l \in Z, 0 \leqslant j \leqslant J-1} \cup \{\phi_{0,k} \otimes \phi_{0,l}\}_{k,l \in Z}.$$

We have used this MRA approach in our two-dimensional problem.

2.3. Convection problem

Consider the convection equation

$$\partial_t u = a \partial_x u, \tag{2.6}$$

where a is positive constant coefficient.

2.3.1. Time discretization

To obtain an improved order of accuracy in Δt we shall apply a Taylor–Galerkin method based on the following Taylor series expansions: let us first leave the spatial variable x continuous and discretize only the time to obtain the Euler scheme

$$\frac{u^{n+1} - u^n}{\Delta t} = v u_{xx}^n + f(x). \tag{2.7}$$

We are expressing the difference approximation to u_t at time level n by forward-time Taylor series expansion, including second and third time derivatives, which gives

$$\frac{u^{n+1}-u^n}{\Delta t} = (u_t)^n + \frac{\Delta t}{2}\,u_{tt}^n + \frac{\Delta t^2}{6}\,u_{ttt}^n + O(\Delta t^3) \tag{2.8}$$

replacing the time derivatives by spatial derivatives, the associated wavelet Taylor–Galerkin equations based on Euler time stepping scheme include high-order time derivatives. While the first-order is provided directly by (2.6) and high-order can be obtained by taking the time derivative of the governing PDEs. We derive two schemes based on the different form of time derivative of Eq. (2.6).

2.3.2. Scheme with a mixed temporal spatial correction (WTGM)

The time derivative of Eq. (2.6) is

$$u_{tt} = a^2 u_{xx} \quad \text{and} \quad u_{ttt} = a^2 (u_t)_{xx} \tag{2.9}$$

and the substitution of Eqs. (2.6) and (2.9) into Taylor series expansion (2.8) gives WTGM scheme

$$Au^{n+1} = Bu^n, \tag{2.10}$$

where

$$A = I - \frac{a^2\delta t^2}{6}\,\partial_x^2 \quad \text{and} \quad B = I - \frac{a^2\delta t^2}{6}\,\partial_x^2 + a\Delta t\partial_x + \frac{a^2\delta t^2}{2}\,\partial_x^2.$$

2.3.3. Scheme with spatial correction (WTGMS)

The time derivative of Eq. (2.6) is

$$u_{tt} = a^2 u_{xx} \quad \text{and} \quad u_{ttt} = a^3 u_{xxx} \tag{2.11}$$

and the substitution of Eqs. (2.6) and (2.11) into Taylor series expansion (2.8) gives WTGMS scheme

$$u^{n+1} = Bu^n, \tag{2.12}$$

where

$$A = I \quad \text{and} \quad B = I + a\delta t\partial_x + \frac{a^2\delta t^2}{2}\,\partial_x^2 + \frac{a^3\delta t^3}{6}\,\partial_x^3.$$

Now wavelet Galerkin discretization turns the problem into a finite-dimensional space.

$$d_u^{n+1} = \mathscr{A}^{-1}\mathscr{B}d_u^n = \mathscr{D}d_u^n. \tag{2.13}$$

In this finite-dimensional space u^n is to be replaced by the vector d_u^n along a wavelet finite basis, and A and B are replaced by, respectively, $\mathscr{A}$ and $\mathscr{B}$ (finite) matrices. Due to second- and third-order term in Taylor series our scheme leads to implicit method that needs inversion. Now to solve Eq. (2.13) on the wavelet basis we will compute $\mathscr{A}^{-1}$ and

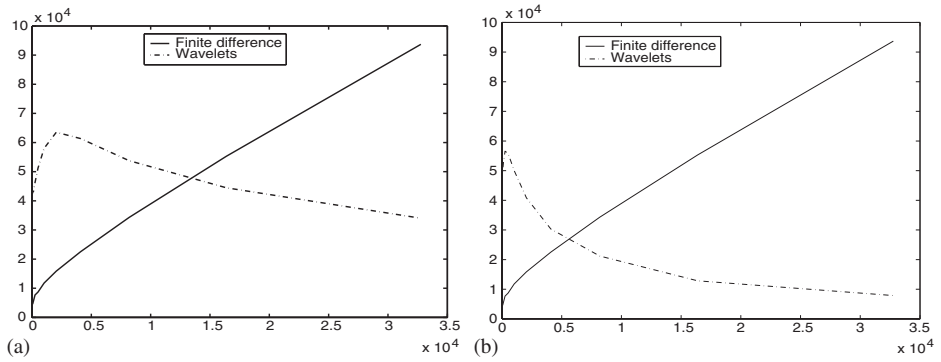

Fig. 1. Number of coefficients in the successive powers D^n: (a) CN times stepping in wavelets and in finite differences, versus $x = 2^n$, $n = 15$, $N = 1024$, $v\delta t = 10^{-5}$, $\varepsilon_M = 10^{-8}$, (b) Taylor–Galerkin approach in wavelets and in finite differences.

$\mathscr{A}^{-1}\mathscr{B}$ once and store in compressed form. We can now give a computational procedure for computing (2.13) using wavelet compression.

Algorithm.

1. $trunc(\mathscr{A}^{-1}, \varepsilon_M)$ - -> $(\mathscr{A}^{-1})^{\varepsilon_M}$,
2. compute initial guess in wavelet basis - -> d_u^0,
3. $trunc(d_u^0, \varepsilon_V)$ - -> $(d_u^0)^{\varepsilon_V}$.
   For $n = 0, 1, \ldots, n1 - 1$,
4. $(\mathscr{A}^{-1})^{\varepsilon_M}\mathscr{B}(d_u^n)^{\varepsilon_V}$ - -> d_u^{n+1},
5. $trunc(d_u^{n+1}, \varepsilon_V)$ - -> $(d_u^{n+1})^{\varepsilon_V}$,
   where $trunc(d_u, \varepsilon_V) = \{d_k^j, \quad |d_k^j| > \varepsilon_V\}$ and $trunc(\mathscr{A}, \varepsilon_M) = \{[A_{m,n}] \quad [A_{m,n}], > \varepsilon_M\}$.

A further property of the wavelet representation of operators is that the successive powers $\mathscr{D}^n$ of the time-iteration matrix become more and more sparser with increasing n. This property is very specific to wavelets, as the opposite occurs with finite difference where $\mathscr{D}^n$ becomes a more and more dense matrix as shown in Fig. 1. It is seen from 1 that in wavelet Taylor–Galerkin approach compression in the matrix D^n is larger than wavelet Galerkin approach. From this property we can obtain iterative speed of the wavelet Taylor Galerkin scheme.

1. Initialize $(\mathscr{A}_0^{-1})^{\varepsilon_M}$ and $(d_u^0)^{\varepsilon_V}$,
2. $(\mathscr{D}_0)^{\varepsilon_M}$ - -> $(\mathscr{A}_0^{-1})^{\varepsilon_M}\mathscr{B}$.
   For $n = 0, 1, \ldots, n1 - 1$,
3. $(\mathscr{D}_n)^{\varepsilon_M}(d_u^n)^{\varepsilon_V}$ - -> $(d_u^{n+1})^{\varepsilon_V}$,
4. $\mathscr{D}_n^2$ - -> $\mathscr{D}_{n+1}$. Then the approximate solution of PDE is at $t = 2^n\delta t$ is $d_u^{(2^n)}$.

Since differential operators are local operators, it seems that not much can be gained by compression. But on a wavelet basis, it is possible to efficiently invert the differential operator and then approximate (in a compressed form) the dense evolution operators. There is no need to change from classical to wavelet coordinates till some time steps. In classical coordinates, the evolution operator changes from very sparse to dense. In the wavelet representation we may start the squaring in the classical coordinates and change to the wavelet basis at the point where the wavelet representation is sparser. Thus, we have the following algorithm:

1. For $n = 0, 2, \ldots, p$,
2. $(A)^{-1} B u^n$ - -> u^{n+1},
3. Initialize $(\mathscr{A}^{-1})^{\varepsilon_V}$ and $(d_u^p)^{\varepsilon_V}$.
   For $n = p+1, p+2, \ldots, p+n1-1$,
4. $(\mathscr{A}^{-1})^{\varepsilon_M} \mathscr{B} (d_u^n)^{\varepsilon_V}$ - -> (d_u^{n+1}),
5. $trunc(d_u^{n+1}, \varepsilon_V)$ - -> $(d_u^{n+1})^{\varepsilon_V}$.

It is essential for the success of this algorithm that the computation of the matrix vector product fully exploits the compressed form of both matrix and vectors. This can be done using the algorithm of [10] or fast multiplication based on a general sparse format for both matrix and vector.

Another wavelet Taylor–Galerkin schemes can also be formulated from the another time stepping, i.e. leap-frog, forward Euler, etc. In all these methods, a fundamental role is played by the Taylor series in the time increment which is exploited indirectly in multi-step schemes and directly in single step ones. In this respect, the two different classes of methods correspond to Runge–Kutta and Obrechkoff [8] methods for ordinary differential equations. WTGM scheme has inconvenience using the higher-order time derivative for calculating nonlinear problems. Therefore, we can also use the following Runge–Kutta form of Lax–Wendroff scheme. By approximating Eq. (2.8) up to third-order accuracy, the formulation of this scheme can be written as

$$\begin{aligned} u^{k+1/3} &= u^k + (\delta t/3) u_t^k, \\ u^{k+1/2} &= u^k + (\delta t/2) u_t^{k+1/3}, \\ u^{k+1} &= u^k + \delta t u_t^{k+1/2}. \end{aligned} \tag{2.14}$$

After putting time derivative from the governing PDEs, spatial discretization of Eq. (2.14) can be performed by wavelet Galerkin method (WGM).

2.3.4. Theoretical stability of the linearized schemes

We use the notion of asymptotic stability of a numerical method as it is defined in [8] for a discrete problem of the form $\mathrm{d}u/\mathrm{d}t = Lu$, where L is assumed to be diagonalization matrix. The region of absolute stability of a numerical method is defined for the scalar model problem $\mathrm{d}u/\mathrm{d}t = \lambda u$ to be set of all $\lambda \delta t$ such that $||u^n||$ is bounded as $t \longrightarrow \infty$. Finally, we say that a numerical method is asymptotic stable for a particular problem if, for small $\delta t > 0$, the product of δt times every eigenvalues of L lies within the region of absolute stability.

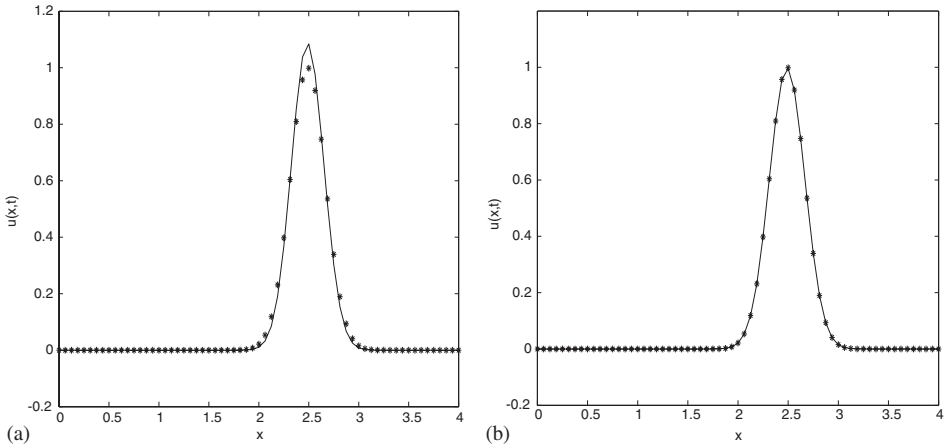

Fig. 2. Solution of convection equation based on Euler time-stepping scheme: (a) WGM scheme, (b) WTGM scheme (-, exact,..., $\Delta t = .01$).

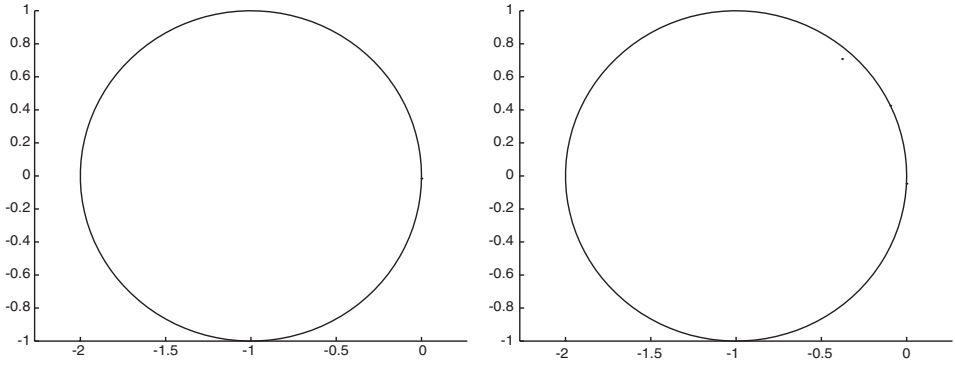

Fig. 3. Absolute stability region for forward Euler and Δt times the eigenvalues of L_j for Daubechies scaling functions, where $\Delta t = .01$, left for $j = 4$, right for $j = 6$.

2.3.5. Numerical results

The accuracy of the proposed WTGM has been verified first on some benchmark problems and later these schemes are applied to turbulent flows where wavelets could be an efficient basis.

2.3.6. Test problem 1

We assume the solution of some large period, for instance, say, four. A comparison of the solution obtained by WGM and WTGM with the exact solution is made in Figs. 2(a and b), respectively illustrates the relative superiority of WTGM with the hyperbolic equation. Fig. 3(a and b) shows the δt times the eigenvalues of matrix resulting from WTGM scheme. The vector $u^{\varepsilon_M,\varepsilon_V}$ is the computed solution given the threshold ε_M and ε_V. Hence, we define

Table 1
Compression error for WGM scheme

$\varepsilon_V = 0$ ε_M	% elem $(\mathscr{A}^{-1})^{\varepsilon_M}$	$E^{\varepsilon_M,\varepsilon_V}$	$\varepsilon_M = 0$ ε_V	% elem $(d_u^n)^{\varepsilon_V}$	$E^{\varepsilon_M,\varepsilon_V}$
10^{-10}	14.74	7.2e − 11	10^{-10}	61.78	5.6e − 10
10^{-9}	14.32	2.2e − 09	10^{-9}	57.81	5.3e − 09
10^{-8}	13.58	8.64e − 09	10^{-8}	56.25	4.5e − 08
10^{-7}	13.18	2.3e − 06	10^{-7}	51.56	3.1e − 07
10^{-6}	11.79	2.21e − 05	10^{-6}	49.21	3.8e − 06

Table 2
Compression error for W-TGM scheme

$\varepsilon_V = 0$ ε_M	% elem $(\mathscr{A}^{-1})^{\varepsilon_M}$	$E^{\varepsilon_M,\varepsilon_V}$	$\varepsilon_M = 0$ ε_V	% elem $(d_u^n)^{\varepsilon_V}$	$E^{\varepsilon_M,\varepsilon_V}$
10^{-10}	18.31	8.6e − 11	10^{-10}	88.28	6.6e − 10
10^{-9}	17.64	6.2e − 10	10^{-9}	85.16	2.4e − 09
10^{-8}	16.88	4.6e − 9	10^{-8}	80.47	3.3e − 08
10^{-7}	15.81	1.3e − 07	10^{-7}	74.22	3.3e − 07
10^{-6}	13.61	2.4e − 05	10^{-6}	67.19	4.7e − 06

the relative compression error as

$$E^{\varepsilon_M,\varepsilon_V} = \frac{\|u^{\varepsilon_M,\varepsilon_V} - u^{0,0}\|_\infty}{\|u^{0,0}\|_\infty}.$$

Tables 1and 2 shows the relative error introduced by compression $E^{\varepsilon_M,\varepsilon_V}$. It is seen in Fig. 1 that a significant compression is achieved in matrix $\mathscr{D}^n$ and in Taylor–Galerkin approach number of elements in matrix $\mathscr{D}^n$ is decaying faster than wavelet Galerkin approach. Here significant compression is also achieved in solution vector.

2.3.7. Test problem 2

The problem of a Gaussian hill translating with a uniform velocity a and spreading isotropically with a diffusivity v has been considered.

$$u_t = -a \cdot \nabla u + v\nabla^2 u. \tag{2.15}$$

Here time discretization will be same as in one-dimensional case as in Eq. (2.6) second-order WTGM scheme. Initial distribution is given in Fig. 4 and the equations are integrated till time $t = .5$ is reached.

2.3.8. Test problem 3

The numerical experiment we present studies the merging of two same sign vortices. It concerns free decaying turbulence (no forcing term). The initial condition for the simulation

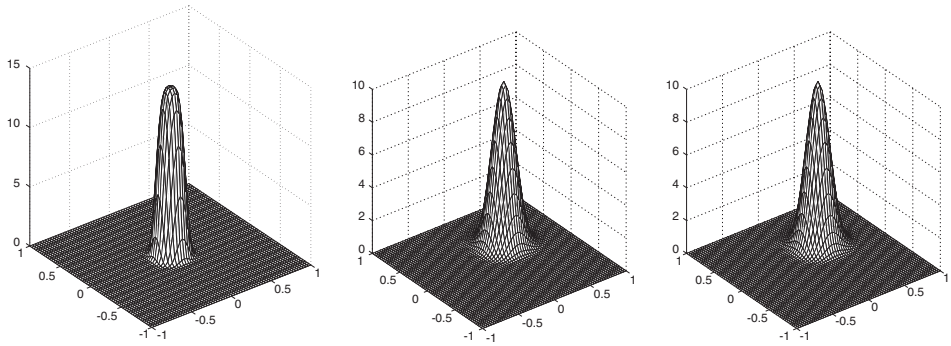

Fig. 4. Initial distribution of the hill (left) and solution at $t = .5$ without compression (in middle) and with compression in (right) for WTGM scheme.

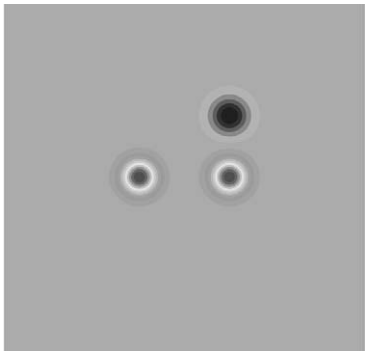

Fig. 5. Three vortex interaction: initial state ($t = 0$).

considered is

$$\omega(x, y) = \sum_{i=1}^{i=3} A_i \exp(-((x - x_i)^2 + (y - y_i)^2)/\sigma_i^2)$$

with variables $\sigma_i = 1/\pi$, amplitudes $A_1 = A_2 = -2A_3 = \pi$, and positions $x_1 = 3\pi/4$, $x_2 = x_3 = 5\pi/4$, $y_1 = y_2 = \pi$, $y_3 = \pi(1 + 1/(9\sigma_2))$. The initial conditions are quite specific, but the general dynamics of the vortex merger should not depend critically on the precise arrangement of the vortices. In fully developed two-dimensional turbulent flows the chance of vortex merging increases with the density of vortices. Here with only three vortices we need this specific configuration to ensure a rapid merger; the negative vortex effectively replaces the mean field which pushes vortices together and induces merging. In fact, the configuration we have chosen should be fairly realistic since in practice mergers are often caused by a fast-moving dipole running into another vortex: this is modeled by the three-vortex initial condition. The initial state is displayed in Fig. 5. In a $2\pi \times 2\pi$ box, three vortices with a Gaussian vorticity profile are present two are positive with the same intensity (π), one is negative with half the intensity of the others.

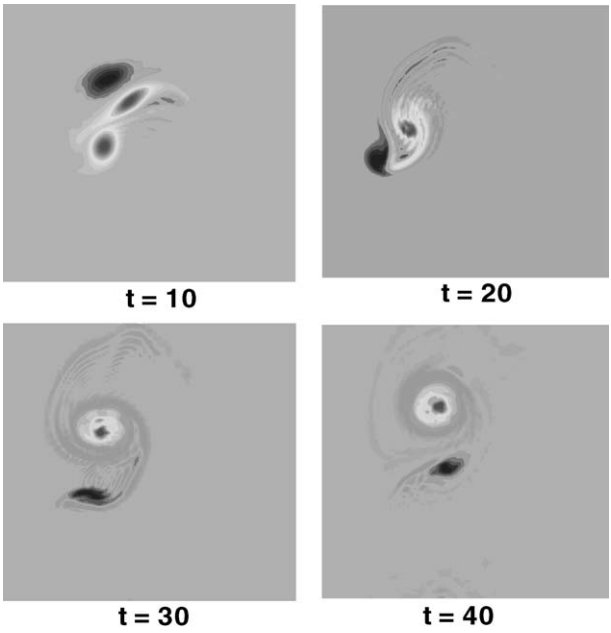

Fig. 6. Vorticity fields at times $t = 10, 20, 30$ and 40.

The maximal scale J is 8, which corresponds to a maximum of $256 \times 256 = 65,536$ degrees of freedom. Further parameters are $\delta t = 2.5 \times 10^{-3}$, $v = 5 \times 10^{-5}$. The turnover time of one of the positive vortices is initially $T = 4.0$, and the initial Reynolds number based on the circulation of one of the positive vortices is $Re = 2 \times 10^4$. Note that since there is no external forcing the energy and enstrophy decay monotonically in time. We determined that the thresholds used in the wavelet compression $\varepsilon_v = 10^{-8}$, $\varepsilon_M = 10^{-8}$ gives satisfactory results. The vorticity fields at times $t = 10$, 20, 30 and 40 are displayed in Fig. 6. The comparison of energy spectra at times $t = 0$, 20 and 40 is shown in Fig. 7.

3. Conclusion

We derived time-accurate wavelet-based schemes for the parabolic and hyperbolic equations. Our time-accurate wavelet-based schemes take advantage of the compression of both the function field and the operator involved, e.g. $(I - \delta t v \partial^2/\partial x^2)^{-1}$, in the wavelet bases in order to simulate two-dimensional turbulence with a reduced number of nonzero elements. The validation of our schemes are presented with the help of convection equation in one dimension and hill translation in two dimension. The schemes have been successfully used in the computational simulation of merging three vortices. The problem of vortex-merging interaction is chosen because it has the strongest nonlinear interaction which is typical of a two-dimensional turbulence.

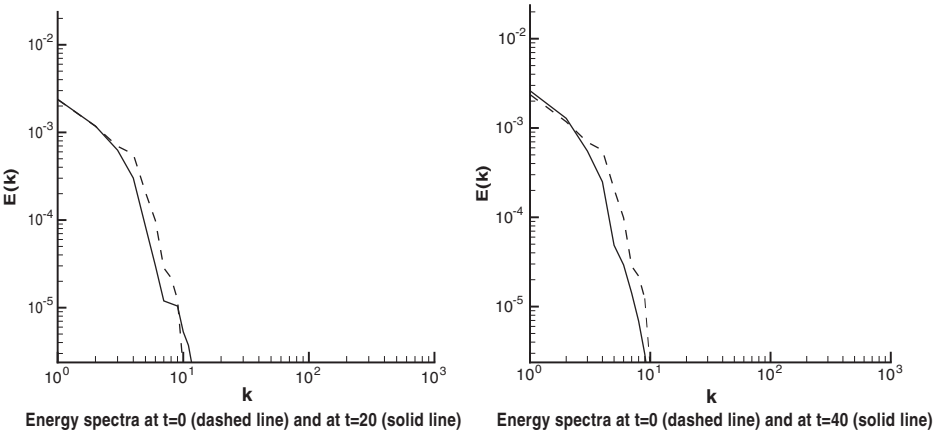

Fig. 7. Comparison of energy spectra at times $t = 0$, 20 and 40.

References

[1] K. Amaratunga, J. Williams, S. Qian, J. Weiss, Wavelet Galerkin solutions for 1D partial differential equations, Int. J. Numer. Math. Eng. 37 (1994) 2703–2716.
[2] A. Cohen, I. Daubechies, J.C. Feauveau, Biorthogonal bases of compactly supported wavelets, Commun. Pure Appl. Math. 45 (1992) 485–560.
[3] I. Daubechies, Orthonormal basis of compactly supported wavelets, Commun. Pure Appl. Math. 41 (1988) 906–966.
[4] D. Donoho, Interpolating wavelet transform, Standford University, 1992, preprint.
[5] B. Engquist, S. Osher, S. Zhong, Fast wavelet based algorithms for linear evolution equations, SIAM J. Sci. Comput. 15 (4) (1994) 755–775.
[6] R. Glowinski, W. Lawton, M. Ravachol, E. Tenenbaum, Wavelet solutions of linear and non-linear elliptic, parabolic and hyperbolic problems in 1D, Computing Methods in Applied Sciences and Engineering, SIAM, PA, 1990, pp. 55–120 (Chapter 4).
[7] L. Jameson, On the wavelet-optimized finite difference method, Technical Report NASA CR-191601, ICASE Report No. 94-9, 1994.
[8] J.D. Lambert, Computational Methods for Ordinary Differential Equations, Wiley, London, 1973.
[9] J. Liandrat, V. Perrier, Ph. Tchmitchian, Numerical resolution of non-linear partial differential equations using wavelet approach, Wavelets and Applications, Boston, MA, 1992, pp. 227–238.
[10] O.M. Nilsen, Wavelets in scientific computing, Ph.D. Thesis, Technical University of Denmark, Lyngby, 1998.
[11] S. Qian, J. Weiss, Wavelets and the numerical solution of partial differential equations, J. Comput. Phys. (1992).